

# Electron-Deficient Early–Late Heterobimetallic Sulfido Clusters. Unusual Reactivities of $\text{Ti}_2\text{Ru}_2\text{S}_4$ Cubane-Type Clusters with Four Cyclopentadienyl Coligands

Shin-ichiro Kabashima, Shigeki Kuwata, and Masanobu Hidai\*

Contribution from the Department of Chemistry and Biotechnology, Graduate School of Engineering, The University of Tokyo, Hongo, Bunkyo-ku, Tokyo 113-8656, Japan

Received January 4, 1999

**Abstract:** Treatment of  $[\text{Cp}_2\text{Ti}(\text{SH})_2]$  (**1**; Cp =  $\eta^5\text{-C}_5\text{H}_5$ ) with  $[(\text{Cp}^*\text{Ru})_4(\mu_3\text{-Cl})_4]$  (**2**; Cp\* =  $\eta^5\text{-C}_5\text{Me}_5$ ) in a Ti:Ru ratio of 1:1 afforded the hydrosulfido-bridged titanium–ruthenium heterobimetallic complex  $[\text{Cp}_2\text{Ti}(\mu_2\text{-SH})_2\text{RuClCp}^*]$  (**3**). Complex **3** reacted with an excess of triethylamine to give the early–late heterobimetallic cubane-type sulfido cluster  $[(\text{CpTi})_2(\text{Cp}^*\text{Ru})_2(\mu_3\text{-S})_4]$  (**4**), with a loss of HCl and cyclopentadiene. An X-ray diffraction study and extended Hückel molecular orbital calculations for the  $60e^-$  cluster **4** demonstrated that **4** has four Ru→Ti dative bonds and a weak Ti–Ti interaction. The reaction of **4** with 3 equiv of  $[\text{Cp}_2\text{Fe}][\text{PF}_6]$  afforded the dicationic cubane-type cluster  $[(\text{CpTi})_2(\text{Cp}^*\text{Ru})_2(\mu_3\text{-S})_4][\text{PF}_6]_2$  (**5**), which contains an additional Ru–Ru bond. In contrast, oxidation of **4** with an excess of HCl at room temperature resulted in the formation of the neutral dichloride cluster  $[(\text{CpTiCl}_2)(\text{CpTi})(\text{Cp}^*\text{Ru})_2(\mu_3\text{-S})_4]$  (**6**). Clusters **5** and **6** were converted into each other by treatment with chloride or hexafluorophosphate anion. Furthermore, substitution of one of the cyclopentadienyl ligands in **6** by a chloride anion took place in boiling 1,2-dichloroethane to give the trichloride cluster  $[(\text{TiCl}_3)(\text{CpTi})(\text{Cp}^*\text{Ru})_2(\mu_3\text{-S})_4]$  (**7**). The detailed structures of these oxidized cubane-type clusters **5**·2DMF, **6**· $\text{CH}_2\text{Cl}_2$ , and **7**· $\text{CH}_2\text{Cl}_2$  as well as the hydrosulfido-bridged dinuclear complex **3** have also been determined by X-ray crystallography. The  $\text{Ti}_2\text{Ru}_2\text{S}_4$  cubane-type cores in **5**–**7** differ considerably in structure from each other, depending upon the ancillary ligands bound to the Ti atoms, although they have a Ru–Ru bond and two Ru→Ti dative bonds in common.

## Introduction

The cubane-type sulfido cluster core,  $\text{M}_4(\mu_3\text{-S})_4$ , is a fundamental structural motif in metal sulfide chemistry.<sup>1–3</sup> It occurs in iron–sulfur proteins, which are involved in a wide range of biological electron-transfer processes,<sup>4</sup> and is also regarded as a molecular counterpart of the nonmolecular cubic lattice known as the rock salt structure. Over the past decade, we have been interested in the reactivities of noble metal centers embedded in metal–sulfur aggregates<sup>5</sup> and have synthesized a number of noble metal sulfido clusters,<sup>6–8</sup> including cubane-type clusters

such as  $[\text{PdMo}_3(\mu_3\text{-S})_4\text{Cl}(\text{tacn})_3]^{3+}$  (tacn = 1,4,7-triazacyclononane)<sup>9</sup> and  $[\{\text{Pd}(\text{PPh}_3)_2\}_2\{\text{Mo}(\text{S}_2\text{CNET}_2)_2\}_2(\mu_3\text{-S})_4]$ .<sup>10</sup> Interestingly, some of these sulfido clusters promote various transformations of organic substrates quite effectively.<sup>9,11</sup> Stimulated by these findings, we envisaged developing the syntheses and reactivities of cubane-type sulfido clusters containing group 4 metals, another class of metals which are biologically unused yet exhibit various reactivities exemplified by polymerization catalysis.<sup>12</sup>

Several synthetic strategies have been established in the preparation of cubane-type sulfido clusters apart from the conventional self-assembly systems. A rational approach involves incorporation of heterometals into the preformed di- or trinuclear metal sulfide aggregates with  $\text{M}_2\text{S}_4$ <sup>13,14</sup> or  $\text{M}_3\text{S}_4$ <sup>3,15</sup> cores. We have successfully applied this method to the prepara-

(1) (a) Dance, I.; Fisher, K. *Prog. Inorg. Chem.* **1994**, *41*, 637–803. (b) Saito, T. In *Early Transition Metal Clusters with  $\pi$ -Donor Ligands*; Chisholm, M. H., Ed.; VCH: New York, 1995; pp 63–164. (c) Lin, Z.; Fan, M.-F. *Struct. Bonding (Berlin)* **1997**, *87*, 35–80.

(2) Harris, S. *Polyhedron* **1989**, *8*, 2843–2882.

(3) (a) Shibahara, T. *Adv. Inorg. Chem.* **1991**, *37*, 143–173. (b) Holm, R. H. *Adv. Inorg. Chem.* **1992**, *38*, 1–71. (c) Shibahara, T. *Coord. Chem. Rev.* **1993**, *123*, 73–147.

(4) *Iron–Sulfur Proteins*; Cammack, R., Ed.; Advances in Inorganic Chemistry 38; Academic Press: New York, 1992.

(5) (a) Hidai, M.; Mizobe, Y.; Matsuzaka, H. *J. Organomet. Chem.* **1994**, *473*, 1–14. (b) Hidai, M.; Mizobe, Y. In *Transition Metal Sulfur Chemistry: Biological and Industrial Significance*; Stiefel, E. I., Matsumoto, K., Eds.; American Chemical Society: Washington, DC, 1996; pp 310–323.

(6) (a) Hashizume, K.; Mizobe, Y.; Hidai, M. *Organometallics* **1996**, *15*, 3303–3309. (b) Tang, Z.; Nomura, Y.; Ishii, Y.; Mizobe, Y.; Hidai, M. *Organometallics* **1997**, *16*, 151–154. (c) Tang, Z.; Nomura, Y.; Ishii, Y.; Mizobe, Y.; Hidai, M. *Inorg. Chim. Acta* **1998**, *267*, 73–79. (d) Kuwata, S.; Andou, M.; Hashizume, K.; Mizobe, Y.; Hidai, M. *Organometallics* **1998**, *17*, 3429–3436.

(7) Tang, Z.; Nomura, Y.; Kuwata, S.; Ishii, Y.; Mizobe, Y.; Hidai, M. *Inorg. Chem.* **1998**, *37*, 4909–4920 and references therein.

(8) (a) Ikada, T.; Kuwata, S.; Mizobe, Y.; Hidai, M. *Inorg. Chem.* **1999**, *38*, 64–69. (b) Amemiya, T.; Kuwata, S.; Hidai, M. *Chem. Commun.* **1999**, 711–712.

(9) Murata, T.; Mizobe, Y.; Gao, H.; Ishii, Y.; Wakabayashi, T.; Nakano, F.; Tanase, T.; Yano, S.; Hidai, M.; Echizen, I.; Nanikawa, H.; Motomura, S. *J. Am. Chem. Soc.* **1994**, *116*, 3389–3398.

(10) Ikada, T.; Kuwata, S.; Mizobe, Y.; Hidai, M. *Inorg. Chem.* **1998**, *37*, 5793–5797.

(11) (a) Wakabayashi, T.; Ishii, Y.; Murata, T.; Mizobe, Y.; Hidai, M. *Tetrahedron Lett.* **1995**, *36*, 5585–5588. (b) Wakabayashi, T.; Ishii, Y.; Ishikawa, K.; Hidai, M. *Angew. Chem., Int. Ed. Engl.* **1996**, *35*, 2123–2124. (c) Nishibayashi, Y.; Yamanashi, M.; Takagi, Y.; Hidai, M. *Chem. Commun.* **1997**, 859–860. (d) Takagi, Y.; Matsuzaka, H.; Ishii, Y.; Hidai, M. *Organometallics* **1997**, *16*, 4445–4452. (e) Masui, D.; Ishii, Y.; Hidai, M. *Chem. Lett.* **1998**, 717–718. (f) Qü, J.-P.; Masui, D.; Ishii, Y.; Hidai, M. *Chem. Lett.* **1998**, 1003–1004.

(12) *Comprehensive Organometallic Chemistry II*; Abel, E. W., Stone, F. G. A., Wilkinson, G., Eds.; Pergamon Press: Oxford, 1995; Vol. 4.

tion of the above-mentioned cubane-type clusters containing noble metals.<sup>8–10</sup> Another rational pathway we have recently developed is  $\alpha$ -dehydrochlorination from hydrosulfido-bridged dinuclear complexes  $[\text{Cp}^*\text{MCl}(\mu_2\text{-SH})_2\text{MCICp}^*]$  ( $\text{M} = \text{Ru}, \text{Rh}, \text{Ir}$ ;  $\text{Cp}^* = \eta^5\text{-C}_5\text{Me}_5$ ), followed by dimerization of the resultant dinuclear  $\text{M}_2(\mu_2\text{-S})_2$  fragments.<sup>6</sup> Quite recently, we have succeeded in extending this methodology to an early–late heterobimetallic system. Thus, the hydrosulfido-bridged heterobimetallic complex  $[\text{Cp}_2\text{Ti}(\mu_2\text{-SH})_2\text{RuClCp}^*]$  (**3**;  $\text{Cp} = \eta^5\text{-C}_5\text{H}_5$ ) has been converted into the heterobimetallic cubane-type sulfido cluster  $[(\text{CpTi})_2(\text{Cp}^*\text{Ru})_2(\mu_3\text{-S})_4]$  (**4**),<sup>16</sup> a still limited example of mixed-metal sulfido clusters containing group 4 metals.<sup>8b,17</sup>

Cubane-type sulfido clusters in which each metal has an  $\eta^5\text{-C}_5\text{R}_5$  coligand have been the subjects for the systematic investigation of the relationship between the number of the total electrons and the metal–metal interactions,<sup>2,6,14,18–25</sup> including the dynamics of the metal–metal bonds without changes in ancillary ligation.<sup>14,24,25</sup> Reactivities of these clusters, however, have been strictly limited to methylation of the bridging sulfur atoms<sup>26</sup> as well as redox reactions owing to the robust  $\text{M}_4(\mu_3\text{-S})_4$  cores surrounded by cyclopentadienyl ligands. In addition, most clusters of this type are homometallic; heterometallic cubane-type sulfido clusters with four cyclopentadienyl ligands remain less common.<sup>2,18</sup> Cluster **4** is notable in containing both electron-deficient group 4 metals and electron-rich group 8 metals in its cubane-type core. We describe here the details of the syntheses and structures of the titanium–ruthenium heterobimetallic cubane-type sulfido cluster **4** and its derivatives. Owing to the sterically and electronically flexible  $\text{Ti}_2\text{Ru}_2(\mu_3\text{-S})_4$  cores, these heterobimetallic sulfido clusters exhibit unusual reactivities at the Ti atom, such as coordination of two further chloro ligands and substitution of the cyclopentadienyl ligand by a chloride anion.

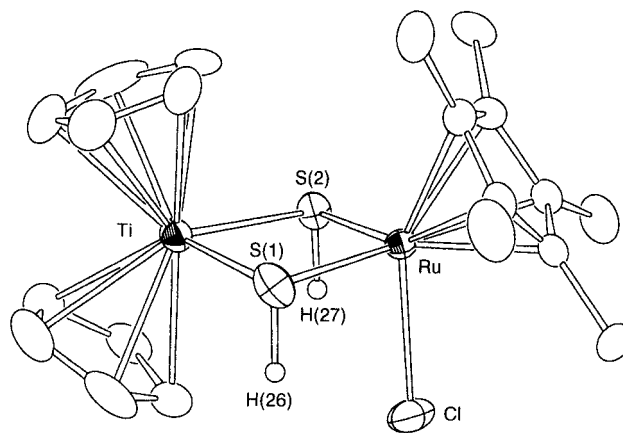
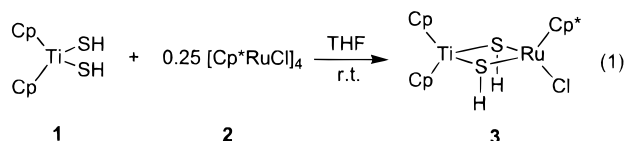


**Figure 1.** Molecular structure of  $[\text{Cp}_2\text{Ti}(\mu_2\text{-SH})_2\text{RuClCp}^*]$  (**3**). Hydrogen atoms except for H(26) and H(27) are omitted for clarity.

## Results and Discussion

**Preparation and Structure of Hydrosulfido-Bridged Heterobimetallic Complex 3.** Adduct formation of hydrosulfido complexes with heterometal complexes is a practical route to mixed-metal hydrosulfido-bridged complexes.<sup>27,28</sup> Thus, we first set about the preparation of hydrosulfido-bridged heterobimetallic complexes corresponding to the homometallic analogues  $[\text{Cp}^*\text{MCl}(\mu_2\text{-SH})_2\text{MCICp}^*]$  ( $\text{M} = \text{Ru}, \text{Rh}, \text{Ir}$ ) by using this method. As expected, the reaction of the “titanadithiol”,  $[\text{Cp}_2\text{Ti}(\text{SH})_2]$  (**1**), with  $[(\text{Cp}^*\text{Ru})_4(\mu_3\text{-Cl})_4]$  (**2**) in a Ti:Ru ratio of 1:1 afforded the hydrosulfido-bridged titanium(IV)–ruthenium(II) complex **3** in good yield (eq 1). It is still to be noted



that the corresponding reactions of organic thiols or hydrogen sulfide with **2** result in cleavage of the S–H bond and oxidation of the ruthenium center, giving the thiolato- or hydrosulfido-bridged diruthenium(III) complexes  $[\text{Cp}^*\text{RuCl}(\mu_2\text{-SR})_2\text{RuClCp}^*]$  ( $\text{R} = \text{Et}, p\text{-C}_6\text{H}_4\text{Me}, \text{H}$ ).<sup>6a</sup> The IR spectrum of **3** exhibits a characteristic weak band at  $2492\text{ cm}^{-1}$ , ascribed to the stretching of the S–H bonds. The presence of hydrosulfido ligands was further confirmed by a hydrosulfido resonance with an intensity of 2H at 2.10 ppm in the  $^1\text{H}$  NMR spectrum. The syn–anti isomerization found in the solutions of many hydrosulfido-bridged dinuclear complexes<sup>6a–c,27,29</sup> was not observed for **3** from  $-50\text{ }^\circ\text{C}$  to room temperature.

The hydrosulfido-bridged heterobimetallic core in **3** has unequivocally been established by X-ray crystallography; the molecular structure of **3** is shown in Figure 1, and selected interatomic distances and angles are listed in Table 1. The structure of **3** closely resembles that of the related thiolato

(27) Ruffing, C. J.; Rauchfuss, T. B. *Organometallics* **1985**, *4*, 524–528.

(28) (a) Küllmer, V.; Vahrenkamp, H. *Chem. Ber.* **1977**, *110*, 3810–3816. (b) Höfler, M.; Hausmann, H.; Heidelberg, H. A. *J. Organomet. Chem.* **1981**, *213*, C1–C3. (c) Challet, S.; Blacque, O.; Gehart, G.; Kubicki, M. M.; Leblanc, J.-C.; Moïse, C.; Brunner, H.; Wachter, J. *New J. Chem.* **1997**, *21*, 903–908.

(29) (a) Küllmer, V.; Vahrenkamp, H. *Chem. Ber.* **1976**, *109*, 1560–1568. (b) Küllmer, V.; Vahrenkamp, H. *Chem. Ber.* **1977**, *110*, 3799–3809. (c) Seyferth, D.; Womack, G. B.; Henderson, R. S.; Cowie, M.; Hames, B. W. *Organometallics* **1986**, *5*, 1568–1575.

(13) (a) Wachter, J. *Angew. Chem., Int. Ed. Engl.* **1989**, *28*, 1613–1626. (b) Zhu, N.; Zheng, Y.; Wu, Z. *J. Chem. Soc., Chem. Commun.* **1990**, 780–781. (c) Diller, H.; Keck, H.; Wunderlich, H.; Kuchen, W. *J. Organomet. Chem.* **1995**, *489*, 123–127. (d) Mansour, M. A.; Curtis, M. D.; Kampf, J. W. *Organometallics* **1997**, *16*, 275–284. (e) Zhu, H.; Liu, Q.; Huang, X.; Wen, T.; Chen, C.; Wu, D. *Inorg. Chem.* **1998**, *37*, 2678–2686.

(14) Feng, Q.; Rauchfuss, T. B.; Wilson, S. R. *J. Am. Chem. Soc.* **1995**, *117*, 4702–4703.

(15) (a) Zhou, J.; Raebiger, J. W.; Crawford, C. A.; Holm, R. H. *J. Am. Chem. Soc.* **1997**, *119*, 6242–6250. (b) Miyake, N.; Imoto, H.; Saito, T. *Chem. Lett.* **1997**, 631–632.

(16) Kuwata, S.; Hiday, M. *Chem. Lett.* **1998**, 885–886.

(17) Casado, M. A.; Ciriano, M. A.; Edwards, A. J.; Lahoz, F. J.; Pérez-Torrente, J. J.; Oro, L. A. *Organometallics* **1998**, *17*, 3414–3416.

(18) Dobbs, D. A.; Bergman, R. G. *Inorg. Chem.* **1994**, *33*, 5329–5336.

(19) Blonk, H. L.; van der Linden, J. G. M.; Steggerda, J. J.; Geleyn, R. P.; Smits, J. M. M.; Beurskens, G.; Beurskens, P. T.; Jordanov, J. *Inorg. Chem.* **1992**, *31*, 957–962.

(20) (a) Pasynskii, A. A.; Eremenko, I. L.; Katugin, A. S.; Gasanov, G. S.; Turchanova, E. A.; Ellert, O. G.; Struchkov, Y. T.; Shklover, V. E.; Berberova, N. T.; Sogomonova, A. G.; Okhlobystin, O. Y. *J. Organomet. Chem.* **1988**, *344*, 195–213. (b) Davies, C. E.; Green, J. C.; Kaltsoyannis, N.; MacDonald, M. A.; Qin, J.; Rauchfuss, T. B.; Redfern, C. M.; Stringer, G. H.; Woolhouse, M. G. *Inorg. Chem.* **1992**, *31*, 3779–3791.

(21) (a) Houser, E. J.; Amarasekera, J.; Rauchfuss, T. B.; Wilson, S. R. *J. Am. Chem. Soc.* **1991**, *113*, 7440–7442. (b) Houser, E. J.; Dev, S.; Ogilvy, A. E.; Rauchfuss, T. B.; Wilson, S. R. *Organometallics* **1993**, *12*, 4678–4681.

(22) (a) Skaugset, A. E.; Rauchfuss, T. B.; Wilson, S. R. *Organometallics* **1990**, *9*, 2875–2876. (b) Feng, Q.; Krautscheid, H.; Rauchfuss, T. B.; Skaugset, A. E.; Venturelli, A. *Organometallics* **1995**, *14*, 297–304.

(23) Herberhold, M.; Jin, G.-X.; Milius, W. *Chem. Ber.* **1995**, *128*, 557–560.

(24) Houser, E. J.; Rauchfuss, T. B.; Wilson, S. R. *Inorg. Chem.* **1993**, *32*, 4069–4076.

(25) Venturelli, A.; Rauchfuss, T. B. *J. Am. Chem. Soc.* **1994**, *116*, 4824–4831.

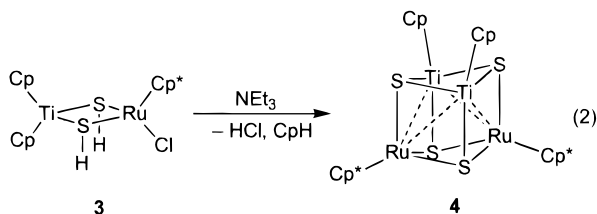
(26) Houser, E. J.; Venturelli, A.; Rauchfuss, T. B.; Wilson, S. R. *Inorg. Chem.* **1995**, *34*, 6402–6408.

**Table 1.** Selected Interatomic Distances and Angles for **3**

Distances (Å)			
Ti–Ru	3.138(1)	Ru–S(1)	2.363(2)
Ru–Cl	2.441(2)	Ru–S(2)	2.361(2)
Ti–S(1)	2.458(2)	S(1)–H(26)	1.20
Ti–S(2)	2.458(2)	S(2)–H(27)	1.13
Angles (deg)			
S(1)–Ti–S(2)	95.87(6)	Ti–S(1)–H(26)	100.4
S(1)–Ru–S(2)	101.15(6)	Ti–S(2)–H(27)	96.0
Ti–S(1)–Ru	81.20(6)	Ru–S(1)–H(26)	98.6
Ti–S(2)–Ru	81.24(6)	Ru–S(1)–H(27)	94.1

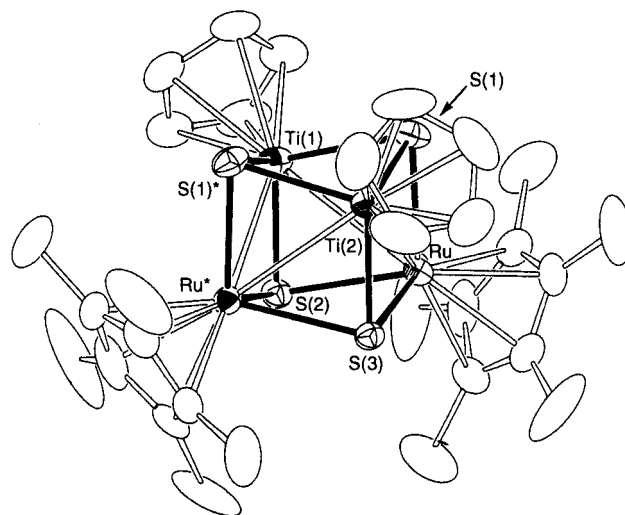
complex [Cp<sub>2</sub>Ti(μ<sub>2</sub>-SPh)<sub>2</sub>RuClCp\*].<sup>30</sup> The final difference Fourier map clearly showed the presence of the two hydrosulfido hydrogen atoms at mutually syn positions, with the S–H distances of 1.20 and 1.13 Å, which is typical in hydrosulfido complexes (1.0–1.4 Å).<sup>31,32</sup> The four-membered TiRuS<sub>2</sub> ring is almost planar, with the dihedral angle of 172.64(9)°, along with the Ti–Ru vector. The Ti–Ru distance of 3.138(1) Å suggests a weak Ti–Ru interaction at most, although the Ti–S–Ru angles (81.2° (mean)) are somewhat small. Complex **3** provides a rare example of structurally characterized hydrosulfido-bridged heterometallic complexes.<sup>28c</sup>

**Conversion of 3 into Heterobimetallic Cubane-Type Sulfido Cluster 4.** Taking account of the facile conversion of homometallic hydrosulfido-bridged dinuclear complexes into cubane-type sulfido clusters with the aid of triethylamine,<sup>6b–d</sup> we treated the heterobimetallic complex **3** in a similar manner. The reaction product exhibits only one Cp and one Cp\* resonances in an intensity ratio of 5:15 in its <sup>1</sup>H NMR spectrum, suggesting the formation of the cubane-type sulfido cluster **4** with a loss of one of the two cyclopentadienyl groups in **3** (eq 2). Indeed, nearly 2 equiv of cyclopentadiene per **4** was detected



in an NMR tube reaction of **3** with triethylamine. Subsequent recrystallization afforded **4** as dark reddish brown crystals in 81% yield. Microanalysis data were also congruent with the formulation of **4** shown in eq 2.

An X-ray analysis has been undertaken to elucidate the detailed structure of **4**; the molecular structure of **4** is depicted in Figure 2, and selected interatomic distances are listed in Table 2. Cluster **4** has a crystallographically imposed mirror plane containing the Ti(1), Ti(2), S(2), S(3), C(1), and C(4) atoms. The Ti–Ru distances of 2.9269(8) and 2.9440(8) Å are considerably longer than those reported so far (2.503(1)–2.663(1) Å),<sup>33</sup> although a certain degree of metal–metal multiple bonding is postulated for the latter distances. The Ti–Ru distances in **4** are, however, still shorter than that in the parent **3** and consistent with a dative bond from the electron-rich Ru atom to the electron-deficient Ti atom, as suggested by extended Hückel molecular orbital (EHMO) calculations (vide infra). The

**Figure 2.** Molecular structure of [(CpTi)<sub>2</sub>(Cp\*Ru)<sub>2</sub>(μ<sub>3</sub>-S)<sub>4</sub>] (**4**). Hydrogen atoms are omitted for clarity.**Table 2.** Selected Interatomic Distances (Å) for **4–7**

	<b>4</b>		<b>5</b> ·2DMF	<b>6</b> ·CH <sub>2</sub> Cl <sub>2</sub>	<b>7</b> ·CH <sub>2</sub> Cl <sub>2</sub>
Ti(1)–Ti(2)	3.060(1)	Ti(1)–Ti(2)	3.105(2)	3.478(2)	3.281(2)
Ti(1)–Ru	2.9440(8)	Ti(1)–Ru(1)	3.002(1)	3.850(2)	3.517(1)
		Ti(1)–Ru(2)	2.964(1)	3.831(2)	3.346(2)
Ti(2)–Ru	2.9269(8)	Ti(2)–Ru(1)	2.975(1)	2.904(2)	2.995(1)
		Ti(2)–Ru(2)	3.003(1)	2.963(2)	2.956(1)
Ru–Ru*	3.547(1)	Ru(1)–Ru(2)	2.8136(8)	2.809(1)	2.8141(8)
Ti(1)–S(1)	2.351(1)	Ti(1)–S(1)	2.323(2)	2.539(3)	2.455(2)
		Ti(1)–S(2)	2.321(2)	2.534(3)	2.408(2)
Ti(1)–S(2)	2.257(2)	Ti(1)–S(3)	2.277(2)	2.570(3)	2.391(2)
Ti(2)–S(1)	2.350(1)	Ti(2)–S(1)	2.316(2)	2.299(3)	2.276(2)
		Ti(2)–S(2)	2.321(2)	2.297(3)	2.282(2)
Ti(2)–S(3)	2.261(2)	Ti(2)–S(4)	2.274(2)	2.277(3)	2.274(2)
Ru–S(1)	2.356(1)	Ru(1)–S(1)	2.409(2)	2.382(2)	2.406(2)
Ru–S(2)	2.3956(9)	Ru(1)–S(3)	2.339(2)	2.315(3)	2.321(2)
Ru–S(3)	2.385(1)	Ru(1)–S(4)	2.335(2)	2.311(2)	2.317(2)
		Ru(2)–S(2)	2.412(2)	2.382(2)	2.409(2)
		Ru(2)–S(3)	2.326(2)	2.316(2)	2.330(2)
		Ru(2)–S(4)	2.337(2)	2.313(3)	2.329(2)
		Ti(1)–Cl(1)		2.407(3)	2.367(2)
		Ti(1)–Cl(2)		2.413(3)	2.329(2)
		Ti(1)–Cl(3)			2.371(2)

Ti–Ti distance (3.060(1) Å) lies in the middle of those in the diamagnetic titanium sulfido clusters with four skeletal electrons [(Cp'Ti)<sub>4</sub>(μ<sub>3</sub>-S)<sub>4</sub>] (2.927(13)–3.008(10) Å; Cp' = η<sup>5</sup>-C<sub>5</sub>H<sub>4</sub>Me)<sup>34</sup> and the nonbonding contacts between sulfido-bridged d<sup>0</sup> titanium centers in [Cp<sub>2</sub>Ti(μ<sub>2</sub>-S)<sub>2</sub>TiClCp],<sup>35</sup> [Cp\*TiX(μ<sub>2</sub>-S)<sub>2</sub>TiXCp\*] (X = Cl, OC<sub>6</sub>H<sub>3</sub>Pr<sup>i</sup>-2,6),<sup>36</sup> [X<sub>2</sub>Ti(μ<sub>2</sub>-S)<sub>2</sub>TiX{η<sup>1</sup>-NC(Ph)N(SiMe<sub>3</sub>)<sub>2</sub>}] (X = PhC(NSiMe<sub>3</sub>)<sub>2</sub>),<sup>37</sup> and [Na<sub>4</sub>(thf)<sub>8</sub>][{(CpTiS)<sub>2</sub>(μ<sub>2</sub>-S)<sub>2</sub>}]<sup>38</sup> (3.127(3)–3.27 Å). These observations suggest the presence of a weak bonding interaction between the Ti atoms in **4**. The Ru–Ru distance at 3.547(1) Å clearly shows the absence of any bonding interactions between these ruthenium centers. This metal–metal bonding scheme for the 60e<sup>−</sup> cluster **4** sharply contrasts with those for other 60e<sup>−</sup> clusters, such as [(η<sup>5</sup>-C<sub>5</sub>H<sub>4</sub>Pr<sup>i</sup>)Mo]<sub>4</sub>(μ<sub>3</sub>-S)<sub>4</sub>,<sup>39</sup> which obey the effective atomic number

(34) Darkwa, J.; Lockemeyer, J. R.; Boyd, P. D. W.; Rauchfuss, T. B.; Rheingold, A. L. *J. Am. Chem. Soc.* **1988**, *110*, 141–149.

(35) Maué, P. G.; Fenske, D. *Z. Naturforsch.*, **B 1988**, *43*, 1213–1218.

(36) Firth, A. V.; Witt, E.; Stephan, D. W. *Organometallics* **1998**, *17*, 3716–3722.

(37) Hagadorn, J. R.; Arnold, J. *Organometallics* **1998**, *17*, 1355–1368.

(38) Lundmark, P. J.; Kubas, G. J.; Scott, B. L. *Organometallics* **1996**, *15*, 3631–3633.

(39) Bandy, J. A.; Davies, C. E.; Green, J. C.; Green, M. L. H.; Prout, K.; Rodgers, D. P. S. *J. Chem. Soc., Chem. Commun.* **1983**, 1395–1397.

(30) Fujita, K.; Ikeda, M.; Nakano, Y.; Kondo, T.; Mitsudo, T. *J. Chem. Soc., Dalton Trans.* **1998**, 2907–2913.

(31) Jessop, P. G.; Lee, C.-L.; Rastar, G.; James, B. R.; Lock, C. J. L.; Faggiani, R. *Inorg. Chem.* **1992**, *31*, 4601–4605.

(32) Liang, H.-C.; Shapley, P. R. *Organometallics* **1996**, *15*, 1331–1333.

(33) Friedrich, S.; Memmler, H.; Gade, L. H.; Li, W.-S.; Scowen, I. J.; McPartlin, M.; Housecroft, C. E. *Inorg. Chem.* **1996**, *35*, 2433–2441.

(EAN) rule and consequently have six metal–metal bonds. The  $\text{Ti}_2\text{Ru}_2(\mu_3\text{-S})_4$  cube in **4** is compressed along with the idealized two-fold axis: the distances of the metal–sulfur bonds perpendicular to the homometallic  $\text{M}_2\text{S}_4$  faces (Ti–S, 2.259; Ru–S, 2.356 Å (mean)) are shorter than those in the homometallic faces (Ti–S, 2.351; Ru–S, 2.390 Å (mean)).

Elimination of cyclopentadiene evidently occurred in the present reaction. Kubas and co-workers have recently reported that deprotonation of **1** with NaH affords the thiotitanate anion  $[\text{Na}_4(\text{thf})_8][\{(\text{CpTiS})_2(\mu_2\text{-S})_2\}_2]$  with a loss of cyclopentadiene.<sup>38</sup> Another closely related reaction is the formation of the titanium–rhodium heterobimetallic sulfido clusters  $[\text{CpTi}(\mu_3\text{-S})_3\{\text{Rh}(\text{CO})_2\}_3]$  and  $[(\text{CpTi})_2\{\text{Rh}(\text{CO})_2\}_2\{\text{Rh}(\text{CO})_2\}_2(\mu_4\text{-O})(\mu_3\text{-S})_4]$  from the reaction of **1** with  $[\{\text{Rh}(\mu_2\text{-OMe})(\text{cod})\}_2]$  (cod = 1,5-cyclooctadiene) under CO, in which cyclopentadiene is believed to be released from the initial intermediate,  $[\text{Cp}_2\text{Ti}(\mu_2\text{-S})(\mu_2\text{-SH})\text{Rh}(\text{cod})]$ .<sup>17</sup> Elimination of cyclopentadiene in these reactions could be categorized into  $\alpha$ -elimination of alkane from alkyl–hydrosulfido complexes, which is exemplified by a thermal loss of methane from the methyl–hydrosulfido complex  $[\text{Ph}_4\text{P}][\text{Ru}(\text{N})\text{Me}_3(\text{SH})]$  to give finally the triruthenium sulfido cluster  $[\text{Ph}_4\text{P}][\{\text{Ru}(\text{N})\text{Me}_2\}_3(\mu_3\text{-S})_2]$ .<sup>32</sup> Thermal elimination of cyclopentadiene and HCl from **3** also took place, although the yield of **4** was somewhat lower. It should be mentioned, however, that treatment of the related hydrosulfido-bridged heterobimetallic complex  $[\text{Cp}_2\text{Ti}(\mu_2\text{-SH})_2\text{Mo}(\text{CO})_4]$  with base resulted in simple deprotonation of the hydrosulfido ligands.<sup>27</sup>

Sulfido clusters of group 4 metals,<sup>1,34,36,40,41</sup> especially those containing heterometals,<sup>8b,17</sup> remain less common compared with the highly prevalent counterparts of group 6 and 8 metals.<sup>42</sup> This is partly due to the lack of a synthetic strategy for the preparation of such clusters, except for a self-assembly approach. As described in the present study, stepwise construction from hydrosulfido-bridged complexes may provide an attractive route to group 4 metal sulfido clusters. Because little is known about such clusters, we have further investigated the electronic structure and reactivities of **4**.

**Electronic Structure of 4.** To gain more insight into the metal–metal interactions in the early–late heterobimetallic cubane-type sulfido cluster **4**, we have performed EHMO calculations for the hypothetical cluster  $[(\text{CpTi})_2(\text{CpRu})_2(\mu_3\text{-S})_4]$  with an idealized  $C_{2v}$  structure based on the crystal structure of **4**. Figure 3 shows the energy level diagram for the low-lying d-type orbitals, which are occupied by the 12 d electrons of the cluster. The most striking feature of the orbital scheme is the localization of these orbitals, predominantly on the two Ru atoms. This localization is ascribed to the mismatch of the energy levels of the Ti and Ru orbitals. However, a significant bonding interaction between the Ti and Ru atoms is still deduced from the overlap populations between these atoms (0.4831). In fact, Figure 3 demonstrates that the  $1a_2$  and  $2a_1$  orbitals have some electron density on the Ti atoms and have a bonding character between the Ti and Ru atoms. This bonding interaction could be described as a dative bond from the electron-rich Ru atom to the electron-deficient Ti atom. In the  $2a_1$  orbital, a weak

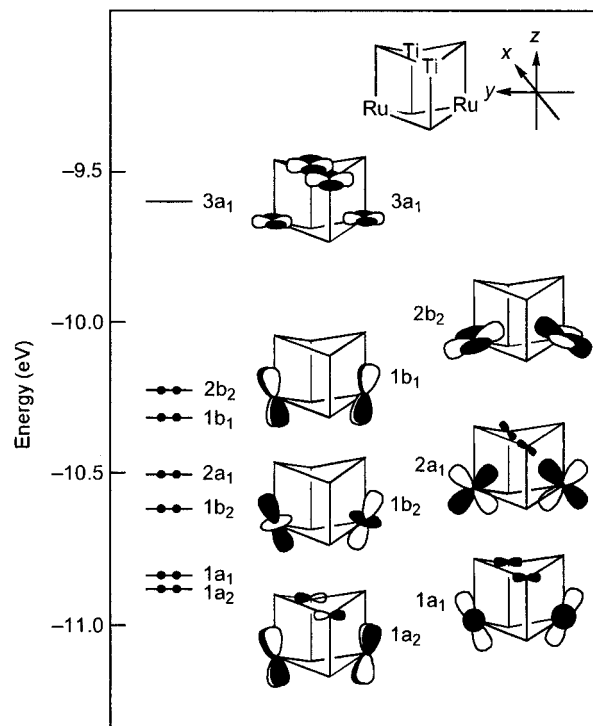


Figure 3. Energy level diagram for  $[(\text{CpTi})_2(\text{CpRu})_2(\mu_3\text{-S})_4]$ .

bonding interaction even between the two Ti atoms is observed. This orbital also has a bonding character between the two Ru atoms, although occupation of the strongly antibonding  $2b_2$  orbital cancels out the bonding interaction. The rest of the occupied orbitals are essentially nonbonding between the metals. These calculation results are in full agreement with the observed structure of **4**.

It is of interest to compare the orbital diagram for the early–late heterobimetallic cluster **4** with those for other cubane-type clusters. In the homometallic cubane-type sulfido clusters of main group metals without d electrons, such as  $[(\text{Me}_2\text{EtC})\text{M}]_4(\mu_3\text{-S})_4$  ( $\text{M} = \text{Al}, \text{Ga}$ )<sup>43</sup> and the halide clusters containing  $d^{10}$  metal centers  $[\{\text{M}(\text{PR}_3)_4(\mu_3\text{-X})\}_4]$  ( $\text{M} = \text{Cu}, \text{Ag}; \text{X} = \text{Cl}, \text{Br}, \text{I}$ ),<sup>44</sup> long metal–metal distances indicating the absence of any bonding between the metal atoms are generally observed, consistent with the electron counts.<sup>45</sup> Aside from these clusters, cubane-type clusters containing  $d^n$  metal centers ( $0 < n < 10$ ) have partially filled d-type orbitals based on the five d orbitals of each metal. In Dahl's qualitative molecular orbital scheme for  $[(\text{CpFe})_4(\mu_3\text{-S})_4]^{n+}$ ,<sup>46</sup> the metal d electrons are delocalized throughout the metal framework. The 20 d-type orbitals for these electrons are categorized into three groups: six metal–metal bonding orbitals, six metal–metal antibonding orbitals, and eight orbitals which are essentially nonbonding between the metal atoms; all of the eight nonbonding orbitals lie above the metal–metal bonding and antibonding orbitals. This bonding scheme has successfully been applied to other homometallic cubane-type clusters in which all four metals have an octahedral environment.<sup>2</sup> For example, the 12 d electrons in the  $60e^-$  cluster  $[(\eta^5\text{-C}_5\text{H}_4\text{Pr}^+)\text{Mo}]_4(\mu_3\text{-S})_4$  occupy the six low-lying metal–metal bonding orbitals, and consequently this cluster has six

(40) (a) Krug, V.; Koellner, G.; Müller, U. *Z. Naturforsch., B* **1988**, *43*, 1501–1509. (b) Cotton, F. A.; Feng, X.; Kibala, P. A.; Sandor, R. B. *W. J. Am. Chem. Soc.* **1989**, *111*, 2148–2151.

(41) (a) Bottomley, F.; Day, R. W. *Can. J. Chem.* **1992**, *70*, 1250–1259. (b) Firth, A. V.; Stephan, D. W. *Inorg. Chem.* **1997**, *36*, 1260–1262. (c) Firth, A. V.; Stephan, D. W. *Organometallics* **1997**, *16*, 2183–2188.

(42) Terminal chalcogenido complexes of group 4 metals have attracted much attention in recent years. See, for example: (a) Parkin, G. *Prog. Inorg. Chem.* **1998**, *47*, 1–165. (b) Sweeney, Z. K.; Polse, J. L.; Andersen, R. A.; Bergman, R. G. *J. Am. Chem. Soc.* **1998**, *120*, 7825–7834.

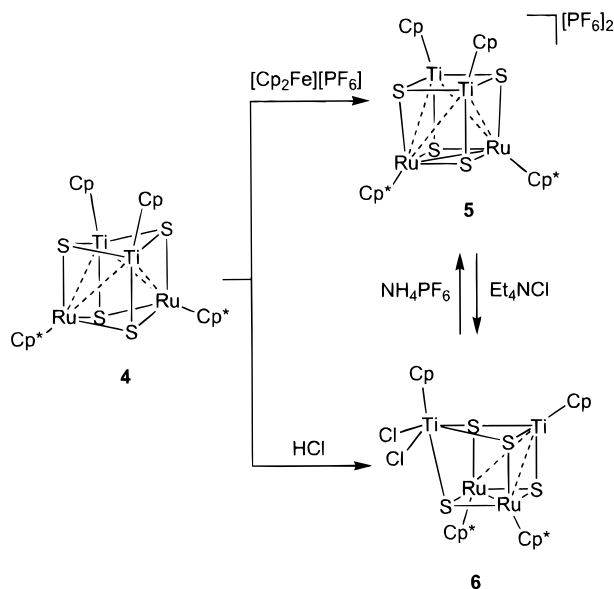
(43) Harlen, C. J.; Gillan, E. G.; Bott, S. G.; Barron, A. R. *Organometallics* **1996**, *15*, 5479–5488.

(44) Teo, B.-K.; Calabrese, J. C. *Inorg. Chem.* **1976**, *15*, 2467–2474.

(45) Dance, I. G. In *Comprehensive Coordination Chemistry*; Wilkinson, G.; Gillard, R. D.; McCleverty, J. A., Eds.; Pergamon Press: Oxford, 1987; Vol. 1, pp 135–177.

(46) Trinh-Toan; Teo, B. K.; Ferguson, J. A.; Meyer, T. J.; Dahl, L. F. *J. Am. Chem. Soc.* **1977**, *99*, 408–416.

## Scheme 1



Mo–Mo bonds.<sup>39</sup> As to heterometallic clusters, Harris and co-workers have recently compared the bonding schemes for the transition metal cubane-type clusters with and without a main group metal.<sup>47</sup> As in the Dahl's scheme, metal d electrons in the Mo<sub>3</sub>Ni cluster  $[\{\text{Mo}(\text{H}_2\text{O})_3\}_3\{\text{Ni}(\text{CO})\}(\mu_3\text{-S})_4]^{4+}$  are delocalized throughout the M<sub>4</sub> tetrahedron, with significant Ni–Mo bonding interactions as well as three Mo–Mo bonds owing to the close energy levels of molybdenum and nickel. By contrast, the terrible mismatch of the Sn 5s orbital and the d-type orbitals in the Mo<sub>3</sub>S<sub>4</sub> fragment in energy causes the complete localization of d-type orbitals on the Mo<sub>3</sub> center and the absence of Sn–Mo bonds in the Mo<sub>3</sub>Sn cluster  $[\{\text{Mo}(\text{NCS})_3\}_3(\text{SnCl}_3)(\mu_3\text{-S})_4]^{6-}$ , in which the Mo<sub>3</sub>S<sub>4</sub> fragment with three Mo–Mo bonds simply acts as a tridentate donor ligand through the three S atoms. The present Ti<sub>2</sub>Ru<sub>2</sub>S<sub>4</sub> cluster **4** lies in the middle of the two extreme situations. Although the occupied d-type orbitals are considerably localized on the Ru atoms owing to the lower energy of the ruthenium d orbitals than the titanium ones, the electrons are still delocalized on the Ti atoms to some extent, implying the presence of a Ru→Ti dative bond.

Occupation of the ruthenium-based nonbonding orbitals causes the electron deficiency of the Ti atoms and leaves some metal–metal bonding orbitals, such as the 3a<sub>1</sub> orbital, unoccupied. We note that similar electron deficiency is found in other M<sub>2</sub>M'<sub>2</sub>S<sub>4</sub> heterometallic cubane-type clusters, such as  $[(\text{Cp}^{\text{Et}}\text{Mo})_2(\text{CoX})_2(\mu_3\text{-S})_4]$  (58e<sup>−</sup>; Cp<sup>Et</sup> = η<sup>5</sup>-C<sub>5</sub>Me<sub>4</sub>Et; X = Cl, I, SPh)<sup>48</sup> and  $[(\text{Cp}^*\text{Mo})_2(\text{FeCl})_2(\mu_3\text{-S})_4]$  (56e<sup>−</sup>),<sup>49</sup> although metal electrons seem to be more delocalized in these clusters. According to Harris's molecular orbital scheme,<sup>2,50</sup> these clusters have four metal–metal nonbonding orbitals below the bonding ones; these nonbonding orbitals are mainly based on the e-like orbitals of the tetrahedral late transition metal centers. Thus, in this case, eight more electrons are required to fill these nonbonding orbitals before the higher metal–metal bonding orbitals are occupied, and eventually 20 d electrons are necessary to form six metal–metal bonds. However, these electron-deficient

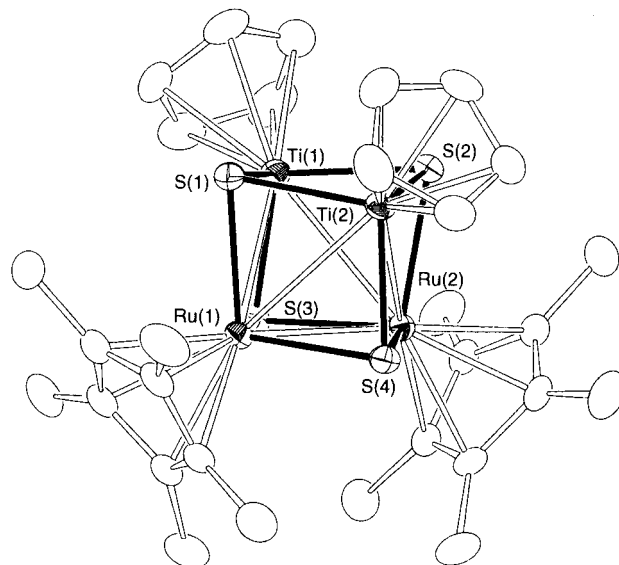


**Figure 4.** Structure of the cationic part in  $[(\text{CpTi})_2(\text{Cp}^*\text{Ru})_2(\mu_3\text{-S})_4][\text{PF}_6]_2 \cdot 2\text{DMF}$  (**5**·2DMF). Hydrogen atoms are omitted for clarity.

clusters have only 18 (in the Mo<sub>2</sub>Co<sub>2</sub> clusters) or 16 (in the Mo<sub>2</sub>Fe<sub>2</sub> cluster) d electrons in their delocalized orbitals and, consequently, have some long M–M contacts due to the partial occupation of the six metal–metal bonding orbitals.

**Oxidation of 4 with Ferrocenium Cation To Give 5.** Because the highest occupied molecular orbital (the 2b<sub>2</sub> orbital) in **4** is antibonding between the two Ru atoms according to the EHMO calculations (vide supra), Ru–Ru bond formation is expected upon oxidation of **4**. The cyclic voltammogram of the cubane-type cluster **4** exhibits two reversible oxidation waves at −0.16 and 0.19 V (vs saturated calomel electrode). In agreement with this, **4** was oxidized with a slight excess of ferrocenium cation to give the two-electron oxidized dicationic cluster **5** in 55% yield (Scheme 1). The <sup>1</sup>H NMR spectrum of **5** again exhibits only one resonance for both Cp and Cp\* protons, indicating that the idealized C<sub>2v</sub> symmetry in **4** is preserved in **5**.

An X-ray analysis of **5** has been carried out to compare the structures of the 60e<sup>−</sup> cluster **4** and the 58e<sup>−</sup> cluster **5** in detail (Figure 4). The asymmetric unit contains two solvating DMF molecules as well as two hexafluorophosphate anions; however, there is no significant interactions between these and the cluster cation. The Ru–Ru distance in **5** (2.8136(8) Å) is considerably shortened from that in **4** (3.547(1) Å), indicating the formation of a Ru–Ru bond upon oxidation. The other metal–metal distances are not affected to a large extent (Table 2). These observations are consistent with the results of the molecular orbital calculations described above. Besides the Ru–Ru distance, the Ti<sub>2</sub>Ru<sub>2</sub>S<sub>4</sub> cubane-type core in **5** differs from that in the parent **4** in some minor points. The distances of the Ru–S bonds parallel to the idealized two-fold axis (2.411 Å (mean)) in **5** are now longer than those in the Ru<sub>2</sub>S<sub>2</sub> face (2.334 Å (mean)). The Ti<sub>2</sub>S<sub>2</sub> and Ru<sub>2</sub>S<sub>2</sub> faces are fairly flattened, with dihedral angles of 162.3 and 172.2° along with the metal–metal vector; the corresponding dihedral angles in **4** are 142.7 and 144.4°, respectively.

**Oxidation of 4 with HCl To Give 6.** When **4** was treated with an excess of HCl gas, two-electron oxidation of **4** also took place. The product **6**, however, has an unexpected structure, with two chloro ligands binding to one of the Ti atoms in the cluster core (Scheme 1).<sup>51</sup> Unlike the case of the dicationic cluster **5**, the <sup>1</sup>H NMR spectrum of **6** exhibits two Cp resonances

(47) Bahn, C. S.; Tan, A.; Harris, S. *Inorg. Chem.* **1998**, *37*, 2770–2778.

(48) Mansour, M. A.; Curtis, M. D.; Kampf, J. W. *Organometallics* **1997**, *16*, 3363–3370.

(49) Kawaguchi, H.; Yamada, K.; Ohnishi, S.; Tatsumi, K. *J. Am. Chem. Soc.* **1997**, *119*, 10871–10872.

(50) Harris, S. *Inorg. Chem.* **1987**, *26*, 4278–4285.

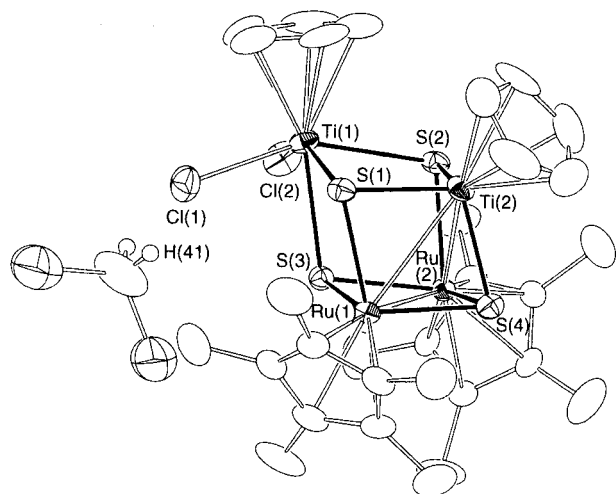


**Figure 5.** Structure of  $[(\text{CpTiCl}_2)(\text{CpTi})(\text{Cp}^*\text{Ru})_2(\mu_3\text{-S})_4]\cdot\text{CH}_2\text{Cl}_2$  (**6** $\cdot\text{CH}_2\text{Cl}_2$ ). Hydrogen atoms except for those in the solvating  $\text{CH}_2\text{Cl}_2$  are omitted for clarity.

along with one  $\text{Cp}^*$  resonance, indicating that the chloro ligands remain to bind to the Ti atom even in the solution. The present reaction sharply contrasts with the exclusive formation of the dicationic clusters  $[(\text{Cp}^*\text{M})_4(\mu_3\text{-S})_4]\text{Cl}_2$  ( $\text{M} = \text{Ru}$ ,<sup>6d</sup>  $\text{Ir}^{25}$ ) upon similar treatment of the homometallic analogues of **4**,  $[(\text{Cp}^*\text{M})_4(\mu_3\text{-S})_4]$ , with  $\text{HCl}$ .

An X-ray analysis has been carried out to clarify the detailed structure of the  $62e^-$  cluster **6**. Figure 5 illustrates the molecular structure of **6** with a considerably distorted cubane-type core. The Ti(1) atom with two chloro ligands extrudes far from the other three metals, with the nonbonding Ti–M ( $\text{M} = \text{Ti}, \text{Ru}$ ) distances of 3.478(2)–3.850(2) Å, whereas the Ru–Ru distance of 2.809(1) Å and the Ti(2)–Ru distances of 2.934 Å (mean) are consistent with a Ru–Ru single bond and Ru→Ti dative bonds, respectively. The Ti(1)–Cl distances (2.410 Å (mean)) are slightly longer than those in  $[\text{Cp}_2\text{TiCl}_2]$  (2.364 Å (mean))<sup>52</sup> but comparable to those in  $[\text{Cp}_2\text{TiCl}_3(\text{dmpe})]$  (2.404 Å (mean);  $\text{dmpe} = \text{Me}_2\text{PCH}_2\text{CH}_2\text{PMe}_2$ ),<sup>53</sup> which has a coordination geometry similar to that in the Ti(1) atom in **6**. Coordination of these two chloro ligands mitigates the electron deficiency of the Ti(1) atom. Indeed, the Ti(1)–S distances at this formally 16-electron Ti(1) center of 2.548 Å (mean) are significantly longer than the corresponding distances at the formally 12-electron Ti(2) center of 2.291 Å (mean); a similar situation is observed in  $[\text{Cp}_2\text{Ti}(\mu_2\text{-S})_2\text{TiClCp}]$ .<sup>35</sup> Cluster **6** may be regarded as a compound which is formally derived from replacement of one of the cyclopentadienyl ligands in titanocene dichloride by a  $\text{TiRu}_2\text{S}_4$  incomplete cubane-type fragment. The distance between the Cl(1) atom in **6** and a hydrogen atom (H(41)) in the solvating dichloromethane molecule is estimated at 2.72 Å, which is slightly shorter than the sum of each van der Waals radius of a hydrogen (1.2 Å) and a chlorine (1.80 Å) atom.<sup>54</sup>

The two oxidized clusters **5** and **6** are easily converted into each other. Treatment of the dicationic cluster **5** with an excess of  $\text{Et}_4\text{NCl}$  afforded the dichloride cluster **6**, whereas addition

(51) This transformation has also been achieved by using concentrated hydrochloric acid instead of  $\text{HCl}$  gas, although the conversion was lower. In this run, concurrent evolution of nearly equimolar amount of hydrogen gas per **6** has been confirmed by GLC analysis.

(52) Clearfield, A.; Warner, D. K.; Saldarriaga-Molina, C. H.; Ropal, R.; Bernal, I. *Can. J. Chem.* **1975**, *53*, 1622–1629.

(53) Hughes, D. L.; Leigh, G. J.; Walker, D. G. *J. Organomet. Chem.* **1988**, *355*, 113–119.

(54) Pauling, L. *The Nature of the Chemical Bond*, 3rd ed.; Cornell University Press: Ithaca, NY, 1960.

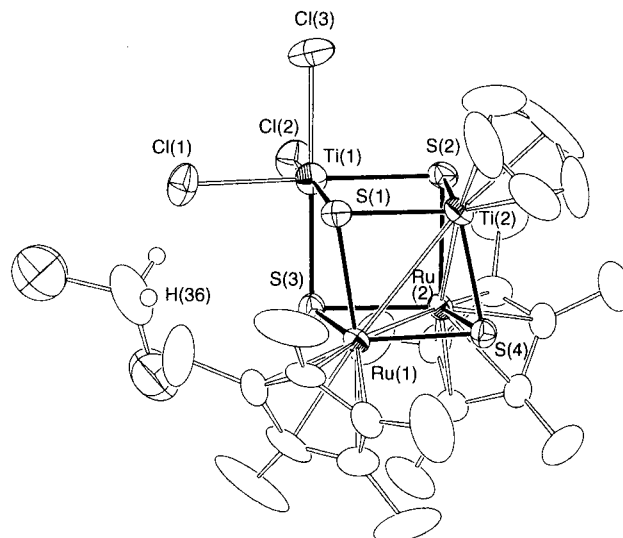
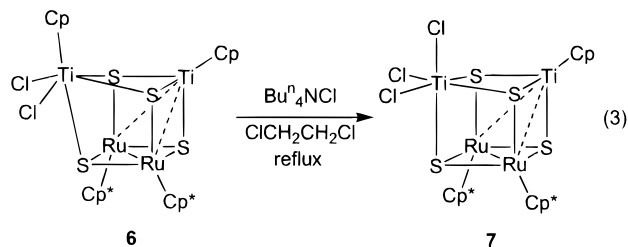


**Figure 6.** Structure of  $[(\text{TiCl}_3)(\text{CpTi})(\text{Cp}^*\text{Ru})_2(\mu_3\text{-S})_4]\cdot\text{CH}_2\text{Cl}_2$  (**7** $\cdot\text{CH}_2\text{Cl}_2$ ). Hydrogen atoms except for those in the solvating  $\text{CH}_2\text{Cl}_2$  are omitted for clarity.

of 2 equiv of  $\text{NH}_4\text{PF}_6$  to the solution of **6** gave **5** (Scheme 1). Facile coordination of chloride anions to the  $\text{Ti}_2\text{Ru}_2(\mu_3\text{-S})_4$  core in **5** represents the flexibility of the cubane-type core. The resultant chloride ligands in **6** are extraordinary labile, as suggested by the long Ti–Cl distances. Such dependence of the cluster cores upon the anions clearly distinguishes the chemistry of the early–late heterobimetallic clusters **5** and **6** from that of the late transition metal clusters having the robust cubane-type  $\{(\eta^5\text{-C}_5\text{R}_5)\text{M}\}_4(\mu_3\text{-S})_4$  cores.

**Substitution of Cyclopentadienyl Ligand in 6 by Chloride Anion To Give 7.** During the study on the reactivities of the titanium–ruthenium sulfido clusters obtained here, we have found the facile substitution of one of the cyclopentadienyl ligands in **6** by a chloride anion. Thus, treatment of **6** with an excess of  $\text{Bu}_4\text{NCl}$  in boiling 1,2-dichloroethane cleanly afforded the trichloride cluster **7** (eq 3). The loss of the cyclopentadienyl



ligand in **6** was deduced from the  $^1\text{H}$  NMR spectrum of **7**, exhibiting one Cp and one  $\text{Cp}^*$  resonances with an intensity ratio of 5:30. The fate of the lost Cp group is, however, unclear at present.

An X-ray analysis has revealed the trichloride structure of the  $58e^-$  cluster **7** (Figure 6). The third chloro ligand completes the  $\text{TiCl}_3\text{S}_3$  octahedral coordination sphere of the cyclopentadienyl-free Ti(1) atom. The Ti(1)–Cl distances in **7** (2.356 Å (mean)) are slightly shortened from those in **6** (2.410 Å (mean)) yet are still considerably longer than those in  $[\text{CpTiCl}_3]$  (2.223 Å (mean)).<sup>55</sup> A solvating dichloromethane molecule again lies close to the cluster molecule, with the shortest estimated contact between the Cl(1) and H(36) atoms of 2.89 Å. Polynuclear titanium–sulfur aggregates with halo ligands themselves are

(55) Engelhardt, L. M.; Papisergio, R. I.; Raston, C. L.; White, A. H. *Organometallics* **1984**, *3*, 18–20.

quite scarce,<sup>40</sup> and cluster **7** is unique in having both a chloride-rich titanium center and firmly bound cyclopentadienyl–metal fragments. Substitution of the cyclopentadienyl ligand on the sulfido cluster by a chloride anion is rather unusual, although formal substitution of cyclopentadienyl ligands in mononuclear titanium complexes by anionic ligands, especially by bidentate ligands, is not unprecedented.<sup>56</sup> For example, conversion of [Cp<sub>2</sub>TiCl<sub>2</sub>] into [CpTiCl<sub>3</sub>] has been achieved by treatment with SO<sub>2</sub>Cl<sub>2</sub> in boiling SOCl<sub>2</sub>.<sup>57</sup>

It is meaningful to compare the structures of the clusters **5**–**7**, which have the same formal oxidation states of the metals but different ancillary ligands on the Ti(1) atoms. The (CpTi)–(Cp\**Ru*)<sub>2</sub>S<sub>4</sub> incomplete cubane-type fragments in these clusters are almost superimposable with each other: the M–M (M = Ti, Ru) distances in this fragment differ by only 0.099 Å at most among these clusters, and the M–S distances also show a small maximum deviation (0.047 Å). In contrast, the Ti(1)–M and Ti(1)–S distances are quite sensitive to the ancillary ligands attached to the Ti(1) atoms, as shown in Table 2. These distances lie in the order of **5** < **7** < **6**. For example, the mean of the Ti(1)–Ru distances ranges from 2.986 Å in the dicationic cluster **5** to 3.841 Å in the dichloride cluster **6**, and the Ti(1)–S(3) distances from 2.276 Å (in **5**) to 2.570 Å (in **6**). The Ti(1)–M and Ti(1)–S distances in the trichloride cluster **7** are located in the middle of those in **5** and **6**.

The TiRu<sub>2</sub>S<sub>4</sub> incomplete cubane-type fragment seems to behave as an “electron sink” to the Ti(1) atom. The order of the bond distances described above reflects that of the electron deficiency at the Ti(1) atoms. This sterically and electronically flexible TiRu<sub>2</sub>S<sub>4</sub> incomplete cubane-type fragment apparently facilitates the unusual substitution of the cyclopentadienyl ligand in **6** by a chloride anion. Thus, the electron deficiency on the formally 12-electron Ti(1) center in **7**, caused by this substitution, is compensated by the donation from the sulfido ligands in this incomplete cubane-type fragment.

## Conclusion

We have demonstrated that synthesis of cubane-type sulfido clusters from hydrosulfido-bridged dinuclear complexes provides an effective method, even in the heterobimetallic system. Facile loss of cyclopentadiene in the conversion of the hydrosulfido-bridged complex **3** into the cubane-type cluster **4** is noteworthy. The resultant early–late heterobimetallic sulfido cluster **4**, a rare example of mixed-metal sulfido clusters containing group 4 metals, has four Ru→Ti dative bonds and a weak Ti–Ti interaction. This bonding scheme sharply contrasts with the presence of six metal–metal bonds in typical 60e<sup>−</sup> homometallic clusters, such as [(η<sup>5</sup>-C<sub>5</sub>R<sub>5</sub>)<sub>4</sub>Mo<sub>4</sub>(μ<sub>3</sub>-S)<sub>4</sub>]. Cluster **4** undergoes two-electron oxidation to give two types of oxidized clusters. One is the dicationic cluster **5**, and the other is the neutral dichloride cluster **6**, with a highly distorted cubane-type core. Notable is the dependence of the core structures upon the anion. Furthermore, unexpectedly facile substitution of the cyclopentadienyl ligand in **6** by a chloride anion takes place to afford the trichloride cluster **7**. These Ti-centered reactivities of the titanium–ruthenium heterobimetallic sulfido clusters are in marked contrast to those of the homometallic cubane-type sulfido clusters of late transition metals with four firmly bound

cyclopentadienyl coligands. It is to be noted that the yields of these reactions are generally high. In the sequentially obtained clusters **4**–**7**, [(Cp<sub>x</sub>TiCl<sub>3</sub>)(CpTi)(Cp\**Ru*)<sub>2</sub>(μ<sub>3</sub>-S)<sub>4</sub>]<sup>n+</sup>, the cubane-type cores deform to a large extent, depending upon the ancillary ligands bound to the electron-deficient Ti atoms, showing the unusual flexibility of the Ti<sub>2</sub>Ru<sub>2</sub>(μ<sub>3</sub>-S)<sub>4</sub> cores. Further study will be directed toward investigation of the reactivities on the titanium centers, especially the trichlorotitanium center in **7**, embedded in the metal–sulfur aggregates.

## Experimental Section

**General Comments.** All manipulations were performed under an atmosphere of nitrogen or argon using standard Schlenk techniques. Solvents were dried by refluxing over Na/benzophenone ketyl (THF, toluene, benzene, hexanes, and diethyl ether), Mg(OMe)<sub>2</sub> (methanol), P<sub>2</sub>O<sub>5</sub> (dichloromethane, 1,2-dichloroethane), CaSO<sub>4</sub> (acetone), or CaH<sub>2</sub> (DMF), and distilled before use. Triethylamine was distilled from KOH. IR spectra were recorded on a Shimadzu 8100M spectrometer. <sup>1</sup>H NMR spectra were recorded on a JEOL EX-270 or LA-400 spectrometers. Hydrogen gas evolution was determined by GLC analysis using a Shimadzu GC-8A gas chromatograph equipped with a Molecular Sieve 13X column. Electrochemical measurements were made with a BAS CV-50W electrochemical analyzer using a glassy carbon working electrode; potentials were measured in CH<sub>2</sub>Cl<sub>2</sub>–0.1 M Bu<sup>n</sup><sub>4</sub>NBF<sub>4</sub> vs a saturated calomel electrode as reference. Elemental analyses were performed on a Perkin-Elmer 2400II CHN analyzer.

**Preparation of [Cp<sub>2</sub>Ti(μ<sub>2</sub>-SH)<sub>2</sub>RuClCp\*] (**3**).** A mixture of **1** (275.3 mg, 1.127 mmol)<sup>58</sup> and **2** (315.3 mg, 0.2901 mmol)<sup>59</sup> was dissolved in THF (20 mL) and was stirred for 10 h. Removal of the solvent and subsequent crystallization from benzene–hexanes (15 mL/40 mL) afforded **3** as dark reddish brown crystals (435.8 mg, 73%). <sup>1</sup>H NMR (CDCl<sub>3</sub>): δ 5.67, 5.14 (s, 5H each, C<sub>5</sub>H<sub>5</sub>), 2.10 (s, 2H, SH), 1.66 (s, 15H, C<sub>5</sub>Me<sub>5</sub>). IR (KBr): 2492 cm<sup>−1</sup> (w, ν<sub>SH</sub>). Anal. Calcd for C<sub>20</sub>H<sub>27</sub>ClRu<sub>2</sub>Ti: C, 46.56; H, 5.27. Found: C, 46.69; H, 5.47.

**Preparation of [(CpTi)<sub>2</sub>(Cp\**Ru*)<sub>2</sub>(μ<sub>3</sub>-S)<sub>4</sub>] (**4**).** (a) To a solution of **3** (1.043 g, 2.021 mmol) in THF (50 mL) was added triethylamine (1.4 mL, 10 mmol) at −78 °C, and the mixture was slowly warmed to room temperature with stirring. After removal of the solvent in vacuo, the resultant reddish brown oil was extracted with benzene. The extract was then chromatographed on alumina with benzene, followed by recrystallization from dichloromethane–methanol (5 mL/45 mL). The dark reddish brown crystals that formed were filtered off and dried in vacuo (675.0 mg, 81%). <sup>1</sup>H NMR (CDCl<sub>3</sub>): δ 5.58 (s, 10H, C<sub>5</sub>H<sub>5</sub>), 1.54 (s, 30H, C<sub>5</sub>Me<sub>5</sub>). Anal. Calcd for C<sub>30</sub>H<sub>40</sub>Ru<sub>2</sub>S<sub>4</sub>Ti<sub>2</sub>: C, 43.58; H, 4.88. Found: C, 43.61; H, 4.95.

(b) A toluene (10 mL) solution of **3** (89.6 mg, 0.174 mmol) was heated at reflux for 7 h. The dark reddish brown solution was evaporated to dryness in vacuo, and the residue was extracted with benzene. The extract was then chromatographed on alumina with benzene. Recrystallization of the reddish brown band from dichloromethane–methanol (1 mL/10 mL) afforded **4** as dark reddish brown crystals (21.8 mg, 30%).

**Preparation of [(CpTi)<sub>2</sub>(Cp\**Ru*)<sub>2</sub>(μ<sub>3</sub>-S)<sub>4</sub>][PF<sub>6</sub>]<sub>2</sub>·DMF (**5**·DMF).** (a) A mixture of **4** (33.1 mg, 0.0400 mmol) and [Cp<sub>2</sub>Fe][PF<sub>6</sub>] (39.6 mg, 0.120 mmol) was dissolved in dichloromethane (10 mL) and stirred for 12 h. The reddish brown precipitate was collected by filtration and recrystallized from DMF–diethyl ether (2 mL/18 mL). The reddish brown crystals that formed were filtered off, washed with diethyl ether, and dried in vacuo (26.3 mg, 55%). <sup>1</sup>H NMR (CD<sub>3</sub>CN): δ 6.57 (s, 10H, C<sub>5</sub>H<sub>5</sub>), 1.73 (s, 30H, C<sub>5</sub>Me<sub>5</sub>). As confirmed by the X-ray analysis, the crystals of **5** obtained here contain two solvating DMF molecules per molecule of **5**. However, the crystals lose one of the solvating molecules when they are thoroughly dried in vacuo. This has been confirmed by obtaining the <sup>1</sup>H NMR spectrum of the dried sample of **5**, and therefore the calculated values in elemental analysis are based

(58) Shaver, A.; Marmolejo, G.; McCall, J. M. *Inorg. Synth.* **1990**, *27*, 65–68.

(59) Fagan, P. J.; Ward, M. D.; Calabrese, J. C. *J. Am. Chem. Soc.* **1989**, *111*, 1698–1719.

(56) (a) Bottrill, M.; Gavens, P. D.; Kelland, J. W.; McMeeking, J. In *Comprehensive Organometallic Chemistry*; Wilkinson, G., Store, F. G. A., Abel, E. W., Eds.; Pergamon: Oxford, 1982; Vol. 3, pp 331–431. (b) For further examples of Cp loss reactions, see: Butts, M. D.; Bergman, R. G. *Organometallics* **1994**, *13*, 1899–1910 and references therein.

(57) Chandra, K.; Sharma, R. K.; Kumar, N.; Garg, B. S. *Chem. Ind. (London)* **1980**, 288.

**Table 3.** X-ray Crystallographic Data for **3**, **4**, **5**·2DMF, **6**·CH<sub>2</sub>Cl<sub>2</sub>, and **7**·CH<sub>2</sub>Cl<sub>2</sub>

	<b>3</b>	<b>4</b>	<b>5</b> ·2DMF	<b>6</b> ·CH <sub>2</sub> Cl <sub>2</sub>	<b>7</b> ·CH <sub>2</sub> Cl <sub>2</sub>
formula	C <sub>20</sub> H <sub>27</sub> ClRuS <sub>2</sub> Ti	C <sub>30</sub> H <sub>40</sub> Ru <sub>2</sub> S <sub>4</sub> Ti <sub>2</sub>	C <sub>36</sub> H <sub>54</sub> F <sub>12</sub> N <sub>2</sub> O <sub>2</sub> P <sub>2</sub> Ru <sub>2</sub> S <sub>4</sub> Ti <sub>2</sub>	C <sub>31</sub> H <sub>42</sub> Cl <sub>4</sub> Ru <sub>2</sub> S <sub>4</sub> Ti <sub>2</sub>	C <sub>26</sub> H <sub>37</sub> Cl <sub>5</sub> Ru <sub>2</sub> S <sub>4</sub> Ti <sub>2</sub>
fw	515.98	826.83	1262.94	982.66	953.02
cryst syst	orthorhombic	orthorhombic	monoclinic	monoclinic	monoclinic
space group	<i>P</i> 2 <sub>1</sub> 2 <sub>1</sub> 2 <sub>1</sub> (No. 19)	<i>Pnma</i> (No. 62)	<i>P</i> 2 <sub>1</sub> / <i>n</i> (No. 14)	<i>P</i> 2 <sub>1</sub> / <i>n</i> (No. 14)	<i>P</i> 2 <sub>1</sub> / <i>n</i> (No. 14)
cryst color	dark red	dark red	dark red	dark brown	dark green
cryst dimens, mm	0.3 × 0.5 × 0.8	0.3 × 0.3 × 0.4	0.2 × 0.2 × 0.5	0.1 × 0.2 × 0.7	0.1 × 0.2 × 0.4
<i>a</i> , Å	15.800(2)	16.799(1)	20.284(4)	10.398(4)	9.857(2)
<i>b</i> , Å	16.424(4)	19.335(2)	11.094(4)	18.263(5)	19.792(2)
<i>c</i> , Å	8.073(2)	10.035(1)	21.909(4)	19.474(4)	17.774(2)
α, deg	90	90	90	90	90
β, deg	90	90	105.36(2)	92.55(3)	91.72(1)
γ, deg	90	90	90	90	90
<i>V</i> , Å <sup>3</sup>	2095.1(6)	3259.4(5)	4753(2)	3694(1)	3465.8(9)
<i>Z</i>	4	4	4	4	4
<i>D</i> <sub>c</sub> , g cm <sup>-3</sup>	1.636	1.685	1.764	1.767	1.826
<i>F</i> (000), e	1048	1664	2536	1968	1896
μ(Mo Kα), cm <sup>-1</sup>	14.30	16.57	12.72	17.56	19.43
reflns measd	+ <i>h</i> , + <i>k</i> , + <i>l</i>	+ <i>h</i> , + <i>k</i> , + <i>l</i>	+ <i>h</i> , + <i>k</i> , ± <i>l</i>	+ <i>h</i> , + <i>k</i> , ± <i>l</i>	+ <i>h</i> , + <i>k</i> , ± <i>l</i>
no. of unique reflns	2148	4202	10 911	8478	7948
transmission factors	0.9502–0.9999	0.6730–0.9983	0.7576–0.9989	0.7414–0.9996	0.9434–0.9998
no. of data used ( <i>I</i> > 3σ( <i>I</i> ))	1919	2723	6494	4063	4714
no. of variables	227	182	560	389	353
<i>R</i> <sup>a</sup>	0.028	0.032	0.046	0.048	0.044
<i>R</i> <sub>w</sub> <sup>a</sup>	0.022	0.024	0.035	0.032	0.034
GOF <sup>b</sup>	2.46	2.70	1.86	1.63	1.60
residual density, e Å <sup>-3</sup>	0.35, -0.54	0.47, -0.39	0.79, -0.60	1.00, -0.99	0.97, -0.68

<sup>a</sup>  $R = \sum ||F_o| - |F_c|| / \sum |F_o|$ ;  $R_w = [\sum w(|F_o| - |F_c|)^2 / \sum w F_o^2]^{1/2}$ ;  $w = [\sigma_c^2(F_o) + p^2 F_o^2 / 4]^{-1}$  ( $p = 0$  (**3**), 0.003 (**4** and **6**·CH<sub>2</sub>Cl<sub>2</sub>), 0.005 (**5**·2DMF), 0.004 (**7**·CH<sub>2</sub>Cl<sub>2</sub>)), with  $\sigma_c(F_o)$  from counting statistics. <sup>b</sup> GOF =  $[\sum w(|F_o| - |F_c|)^2 / (N_{obs} - N_{params})]^{1/2}$ .

on the formula with one solvating DMF. Anal. Calcd for C<sub>33</sub>H<sub>47</sub>F<sub>12</sub>-NOP<sub>2</sub>Ru<sub>2</sub>S<sub>4</sub>Ti<sub>2</sub>: C, 33.31; H, 3.98; N, 1.18. Found: C, 33.06; H, 4.10; N, 1.51.

(b) A mixture of **6**·CH<sub>2</sub>Cl<sub>2</sub> (69.3 mg, 0.0705 mmol) and NH<sub>4</sub>PF<sub>6</sub> (23.1 mg, 0.142 mmol) was dissolved in acetone (10 mL), and the mixture was stirred for 1.5 h. After the white precipitate was filtered off, the reddish brown filtrate was evaporated to dryness in vacuo and washed with water (2 mL × 3) and diethyl ether (2 mL × 3). Recrystallization of the resultant dark reddish brown solid from DMF–diethyl ether (2 mL/18 mL) afforded **5**·DMF as reddish brown crystals (42.3 mg, 50%).

**Preparation of [(CpTiCl<sub>2</sub>)(CpTi)(Cp\**Ru*)<sub>2</sub>(μ<sub>3</sub>-S)<sub>4</sub>]·CH<sub>2</sub>Cl<sub>2</sub> (**6**·CH<sub>2</sub>Cl<sub>2</sub>).** (a) Through a toluene (10 mL) solution of **4** (149.5 mg, 0.1808 mmol) was bubbled HCl gas for 2 min, and the mixture was stirred for 23 h under a HCl pressure slightly higher than 1 atm. The dark red suspension was evaporated to dryness in vacuo, and the resultant black powder was recrystallized from dichloromethane–hexanes (8 mL/12 mL). The black crystals that formed were filtered off and dried in vacuo (145.8 mg, 82%). <sup>1</sup>H NMR (CDCl<sub>3</sub>): δ 6.58, 5.92 (s, 5H each, C<sub>5</sub>H<sub>5</sub>), 1.70 (s, 30H, C<sub>5</sub>Me<sub>5</sub>). Anal. Calcd for C<sub>31</sub>H<sub>42</sub>Cl<sub>4</sub>Ru<sub>2</sub>S<sub>4</sub>Ti<sub>2</sub>: C, 37.89; H, 4.31. Found: C, 37.55; H, 4.25.

(b) A suspension of **5**·DMF (51.5 mg, 0.0433 mmol) and Et<sub>4</sub>NCl (49.0 mg, 0.296 mmol) in toluene (5 mL) was stirred for 17 h and filtered. Evaporation of the solvent from the dark brown filtrate and subsequent recrystallization from dichloromethane–hexanes (1 mL/19 mL) afforded **6**·CH<sub>2</sub>Cl<sub>2</sub> as black crystals (19.1 mg, 45%).

**Preparation of [(TiCl<sub>3</sub>)(CpTi)(Cp\**Ru*)<sub>2</sub>(μ<sub>3</sub>-S)<sub>4</sub>]·CH<sub>2</sub>Cl<sub>2</sub> (**7**·CH<sub>2</sub>Cl<sub>2</sub>).** A solution of **6**·CH<sub>2</sub>Cl<sub>2</sub> (39.9 mg, 0.0406 mmol) and Bu<sub>4</sub>NCl (55.7 mg, 0.200 mmol) in 1,2-dichloroethane (10 mL) was heated at reflux for 24 h. The resultant dark green-brown solution was evaporated to dryness in vacuo, and the residue was recrystallized from dichloromethane–diethyl ether (4 mL/15 mL). The dark green crystalline solid that formed was washed with THF (1 mL × 2) and dried in vacuo (18.8 mg, 49%). <sup>1</sup>H NMR (CDCl<sub>3</sub>): δ 6.12 (s, 5H, C<sub>5</sub>H<sub>5</sub>), 1.75 (s, 30H, C<sub>5</sub>Me<sub>5</sub>). Anal. Calcd for C<sub>26</sub>H<sub>37</sub>Cl<sub>5</sub>Ru<sub>2</sub>S<sub>4</sub>Ti<sub>2</sub>: C, 32.77; H, 3.91. Found: C, 32.37; H, 4.10.

**X-ray Diffraction Studies.** Single crystals suitable for X-ray analyses were sealed in glass capillaries under an inert atmosphere and mounted on a Rigaku AFC7R four-circle diffractometer equipped with a graphite-monochromatized Mo Kα source (λ = 0.7107 Å). Orientation matrices and unit cell parameters were determined by least-squares

**Table 4.** Atomic Parameters Used in the Extended Hückel Calculations<sup>a</sup>

atom	orbital	<i>H</i> <sub>ii</sub> (eV)	ξ <sub>1</sub>	<i>C</i> <sub>1</sub>	ξ <sub>2</sub>	<i>C</i> <sub>2</sub>
H	1s	-13.60	1.300			
C	2s	-21.40	1.625			
	2p	-11.40	1.625			
S	3s	-20.00	1.817			
	3p	-13.30	1.817			
Ti	4s	-8.97	1.075			
	4p	-5.44	0.675			
	3d	-10.81	4.550	0.4206	1.40	0.7839
Ru	5s	-8.31	2.078			
	5p	-3.28	2.043			
	4d	-10.74	5.378	0.5340	2.303	0.6365

<sup>a</sup> Double-ξ functions are used for the transition metals.

treatment of 25 machine-centered reflections with 25° < 2θ < 40°. The data collection was performed at room temperature using the ω–2θ scan technique at a rate of 32 deg min<sup>-1</sup> to a maximum 2θ value of 50° (for **3**) or 55° (all except for **3**). The intensities of three check reflections were monitored every 150 reflections during data collection, which revealed no significant decay, except for **7**. For **7**·CH<sub>2</sub>Cl<sub>2</sub>, a steady decrease (3.2%) of the intensities was observed, and a correction for the decay was applied. Intensity data were corrected for Lorentz-polarization effects and for absorption (*ψ* scans). Details of crystal and data collection parameters are summarized in Table 3.

Structure solution and refinements were carried out by using the teXsan program package.<sup>60</sup> The heavy-atom positions were determined by direct method program (SIR92,<sup>61</sup> for **5**·2DMF) or Patterson method program (DIRDIF92-PATY,<sup>62</sup> except for **5**·2DMF), and remaining non-hydrogen atoms were found by subsequent Fourier syntheses. All non-hydrogen atoms were refined anisotropically by full-matrix least-squares techniques (based on *F*). The hydrogen atoms of the hydro-

(60) *teXsan: Crystal Structure Analysis Package*; Molecular Structure Corp.: The Woodlands, TX, 1985 and 1992.

(61) Altomare, A.; Cascarano, G.; Giacovazzo, C.; Guagliardi, A.; Burla, M. C.; Polidori, G.; Camalli, M. *J. Appl. Crystallogr.* **1994**, *27*, 435.

(62) PATY: Beurskens, P. T.; Admiraal, G.; Beurskens, G.; Bosman, W. P.; Garcia-Granda, S.; Gould, R. O.; Smits, J. M. M.; Smykalla, C. *The DIRDIF program system*; Technical Report of the Crystallography Laboratory, University of Nijmegen: The Netherlands, 1992.



sulfido ligands in **3** were found in the final difference Fourier map, while all other hydrogen atoms were placed at calculated positions; these hydrogen atoms were included in the final stages of refinements with fixed parameters. The absolute structure of **3** was determined by comparison of the *R* and *R<sub>w</sub>* values as well as the goodness-of-fit factors of the enantiomorphs. The atomic scattering factors were taken from ref 63, and anomalous dispersion effects were included; the values of  $\Delta f'$  and  $\Delta f''$  were taken from ref 64.

**Molecular Orbital Calculations.** All molecular orbital calculations were performed on a CAChe system by using the extended Hückel method. The atomic parameters were taken from the literature<sup>65</sup> and are listed in Table 4.

---

(63) *International Tables for X-ray Crystallography*; Kynoch Press: Birmingham, England, 1974; Vol. IV.

(64) *International Tables for X-ray Crystallography*; Kluwer Academic Publishers: Boston, MA, 1992; Vol. C.

**Acknowledgment.** This work was supported by a Grant-in-Aid for Specially Promoted Research (Grant No. 09102004) from the Ministry of Education, Science, Sports, and Culture of Japan.

**Supporting Information Available:** Table of crystal data, atomic coordinates, bond lengths and angles, and anisotropic thermal parameters for **3**, **4**, **5**·2DMF, **6**·CH<sub>2</sub>Cl<sub>2</sub>, and **7**·CH<sub>2</sub>Cl<sub>2</sub> (PDF). This material is available free of charge via the Internet at <http://pubs.acs.org>.

JA990034A

---

(65) (a) Hoffmann, R.; Minot, C.; Gray, H. B. *J. Am. Chem. Soc.* **1984**, *106*, 2001–2005. (b) Jiang, Y.; Tang, A.; Hoffmann, R.; Huang, J.; Lu, J. *Organometallics* **1985**, *4*, 27–34. (c) Tatsumi, K.; Nakamura, A.; Hofmann, P.; Stauffert, P.; Hoffmann, R. *J. Am. Chem. Soc.* **1985**, *107*, 4440–4451.